Biogeosciences Discuss., https://doi.org/10.5194/bg-2018-89
Manuscript under review for journal Biogeosciences
Discussion started: 20 February 2018

Biogeosciences Discussions
Open Access
EGU

Mechanisms of northern North Atlantic biomass variability

Galen A. McKinley[1,2], Alexis L. Ritzer[1], and Nicole S. Lovenduski[3]

[1]Department of Atmospheric and Oceanic Sciences, University of Wisconsin—Madison, Wisconsin, USA
[2]now at Columbia University and Lamont Doherty Earth Observatory, New York, USA
[3]Department of Atmospheric and Oceanic Sciences and Institute of Arctic and Alpine Research, University of Colorado Boulder, Colorado, USA
Correspondence to: Galen A. McKinley (mckinley@ldeo.columbia.edu)

Abstract. In the North Atlantic Ocean north of 40 ºN, intense biological productivity occurs to form the base of a highly productive marine food web. SeaWiFS satellite observations indicate trends of biomass in this region over 1998-2007. Significant biomass increases occur in the northwest subpolar gyre and there are simultaneous significant declines to the east of 30-35 ºW. In this study, we use a regional biogeochemical model of the North Atlantic that captures the observed trends to determine their mechanistic drivers. Biomass increases in the northwest are due to a weakening of the subpolar gyre and associated shoaling of mixed layers that relieves light limitation. Biomass declines to the east of 30-35 ºW are due to reduced horizontal convergence of phosphate. This reduced convergence is attributable to declines in vertical phosphate supply in the regions of deepest winter mixing that lie to the west of 30-35 ºW. Over the full timeframe of the model experiment, 1949-2009, variability of both horizontal and vertical phosphate supply drive variability in biomass on the northeastern flank of the subtropical gyre. In the northeast subpolar gyre horizontal fluxes drive biomass variability for both timeframes. Though physically-driven changes in nutrient supply or light availability are the ultimate drivers of biomass changes, clear mechanistic links between biomass and standard physical variables or climate indices remain largely elusive.

Biogeosciences Discuss., https://doi.org/10.5194/bg-2018-89
Manuscript under review for journal Biogeosciences
Discussion started: 20 February 2018

1 Introduction

Surface ocean phytoplankton are the single largest biomass pool on Earth, form the base of the oceanic food web, and contribute to ocean sequestration of carbon dioxide. The North Atlantic north of 40 °N experiences a strong annual cycle of productivity that is controlled by both light and nutrient limitation.

In general terms, marine phytoplankton growth is limited by nutrients in the subtropics and by light at subpolar latitudes [Fay and McKinley, 2017]. In the subtropics, an enhanced bloom occurs with relief of nutrient stress when vertical mixing is enhanced. In contrast, subpolar regions should have a reduced bloom with enhanced mixing because mixing enhances light limitation. Sverdrup [1953] used observations from a weather ship in the Norwegian Sea to propose the notion of a "critical depth" for subpolar regions. When the mixed layer reaches below the critical depth, physical mixing cycles phytoplankton through dark regions at depth which increases light limitation and decreases production. Dutkiewicz et al. [2001] and Follows and Dutkiewicz [2002] directly characterize productivity drivers with the ratio of the spring critical depth to the winter mixed layer depth in a theoretical model and compare to observations. Their relationships most accurately represent satellite and *in situ* observations in the North Atlantic subtropics and are less predictive in the subpolar gyre. Also identified is an intergyre region where observed relationships do not fit a their conceptual model, presumably because both nutrient and light limitation are of first-order importance.

In recent decades, ocean color satellites have allowed for synoptic assessments of surface ocean productivity and its variability [Yoder and Kennelly, 2003; McClain et al., 2004; Siegel et al., 2005]. The first few years of data from the satellite Sea-viewing Wide Field-of-view Sensor (SeaWiFS) indicated that the seasonal cycle of productivity is largely consistent with the Sverdrup hypothesis [Siegel et al. 2002]. Longer records of ocean color have revealed large-scale interannual changes in ocean productivity in each gyre. Explanations for multi-year changes, and by extension expected future trends with climate warming [Bopp et al., 2013], tend also to be based on the simple Sverdrup hypothesis. For example, multiple analyses suggest that increased stratification due to ocean warming limits the vertical supply of nutrients to the surface ocean and thus causes reductions in productivity [Behrenfeld et al. 2006; Polovina et al. 2008; Martinez et al. 2009]. However, these studies have been refuted in the North Atlantic and the North Pacific subtropics, evidenced by the fact that interannual variability in stratification is uncorrelated with that of productivity, and thus do not support a one-dimensional mixing-productivity framework [Lozier et al. 2011, Dave and Lozier 2010, 2013]. In contrast, large-scale correlations between chlorophyll and sea surface temperature (SST, a proxy for stratification) at low and mid latitudes have been shown to be strongly associated with advective processes in the equatorial Pacific [Dave and Lozier, 2015].

Thus, there is growing evidence that vertical processes alone are not sufficient to explain productivity variability. At the same time, there is evidence that horizontal physical processes could play a role, particularly in the northern subtropical gyre or "intergyre" region of the North Atlantic [Williams and Follows, 1998; Dutkiewicz et al. 2001; Follows and Dutkiewicz 2002; Oschlies 2002; McGillicuddy et al. 2003; Dave et al. 2015].

Biogeosciences Discuss., https://doi.org/10.5194/bg-2018-89
Manuscript under review for journal Biogeosciences
Discussion started: 20 February 2018

Williams and Follows [1998] illustrate that on the mean, horizontal Ekman fluxes are critical to surface nutrient supply in the North Atlantic from 40-60 ºN. However, Williams et al. [2000] find variability of horizontal fluxes to be an order of magnitude smaller than convective flux variability, and thus conclude that vertical processes dominate anomalies. Considering deeper processes, Williams et al. [2006] compare the magnitude of Ekman upwelling to the three-dimensional movement of volume or nutrients from the permanent thermocline to the full mixed layer, or "induction". Climatologically, nutrient supply to the subpolar gyre by induction is many times larger than the supply by Ekman upwelling. Induction is how the "nutrient stream" [Pelegrí et al., 1996; Palter et al., 2005; Williams et al., 2006] is accessed to allow for large-scale supply of nutrients from outside to inside the subpolar gyre. To our knowledge, interannual variability in induction has not been discussed in the literature. Further consideration of both horizontal and vertical processes is warranted with respect to understanding of temporal variability in surface ocean productivity in the North Atlantic.

Changing ocean circulation should influence horizontal and vertical transports of nutrients in the northern North Atlantic. A slowdown of the gyre should relax isopycnal slopes and decrease geostrophic advection along isopycnals. The North Atlantic subpolar gyre has exhibited substantial change since the 1950s when regular observations began to be available [Lozier et al. 2008]. There is evidence these changes occur in response to changing buoyancy forcing and wind stress, in turn associated with modes of climate variability, specifically the North Atlantic Oscillation and East Atlantic Pattern [Häkkinen and Rhines, 2004; Hátún et al., 2005; Lozier et al., 2008; Foukal and Lozier, 2017]. Via Ekman processes, reduction in wind stress should directly reduce upwelling in the subpolar gyre and also the horizontal transport of nutrients [Williams et al. 2000; Dave et al. 2015]. Buoyancy and turbulent fluxes also impact mixed layer depths and influence bloom timing and strength [Bennington et al. 2009]. Consistent with this expectation, links between physical changes in the subpolar gyre and *in situ* observed changes in nutrients and ecosystems at several subpolar timeseries sites have been suggested [Johnson et al. 2013, Hátún et al. 2016, 2017].

In this study, we use a regional model to illustrate how changing light limitation and changing vertical and horizontal nutrient supply led to the significant changes in surface ocean biomass that were observed by SeaWiFS over 1998-2007 in the North Atlantic north of 40º N (Figure 1c).

2 Methods

2.1 Satellite biomass

Our analysis focuses on the period 1998-2007. Monthly SeaWiFS data becomes inconsistent beginning in 2008. For study of interannual trends, avoiding the need to fill gaps in the record is desirable. For additional comparison and extension of the record, biomass estimated from MODIS for 2003-2015 is also presented, again selecting years for which all months are available. For both SeaWiFS and MODIS, biomass is estimated using the updated CbPM algorithm [Westberry et al. 2008] by the Ocean Productivity Group at

Biogeosciences Discuss., https://doi.org/10.5194/bg-2018-89
Manuscript under review for journal Biogeosciences
Discussion started: 20 February 2018

Oregon State University (http://www.science.oregonstate.edu/ocean.productivity/index.php, SeaWiFS downloaded 11.28.16; MODIS downloaded 1.24.18).

2.2 Regional hindcast model

The Massachusetts Institute of Technology General Circulation Model configured for the North Atlantic (MITgcm.NA) [Marshall et al., 1997a; Marshall et al., 1997b], is used. The model domain extends from 20 °S to 81.5 °N, with a horizontal resolution of 0.5° x 0.5° and a vertical resolution of 23 levels that have a thickness of 10 m at the surface and gradually become coarser to 500 m thickness intervals for depth levels deeper than 2200m. NCEP/NCAR Reanalysis I daily wind, heat, freshwater, and radiation fields from 1948-2009 force the model [Kalnay et al., 1996]. To correct for uncertainties in air-sea fluxes, SST and SSS (sea surface salinity) are relaxed to monthly historical SST [Had1SSTv1.0, Rayner et al., 2003] and climatological SSS [Antonov et al. 2006] observations, on the timescale of 2 and 4 weeks, respectively [Ullman et al. 2009]. To characterize sub-grid-scale processes, the Gent-McWilliams [Gent and McWilliams, 1990] eddy parameterization, the KPP boundary layer mixing schemes [Large et al., 1994], and Fox-Kemper et al. [2008] submesoscale physical parameterization are used. The phosphorus-based ecosystem is parameterized following Dutkiewicz et al. [2005], and with modest revisions by Bennington et al. [2009]. This ecosystem has one zooplankton class and two phytoplankton classes ("large" diatoms and "small"). The biogeochemical model explicitly cycles phosphorus, silica and iron, and complete carbon chemistry is also included. This model is identical to the one presented in Breeden and McKinley [2016], and uses the same biogeochemical code as Bennington et al. [2009], Ullman et al. [2009] and Koch et al. [2009].

The coupled model has previously been shown to capture the timing and magnitude of the subpolar spring bloom chlorophyll and its variability as observed by SeaWiFS [Bennington et al. 2009]. Mixed layer depths, carbon system variables and nutrients are well simulated at Bermuda and in the northwest subpolar gyre [Ullman et al. 2009; Koch et al. 2009]. As is common to this type of moderate-resolution model, productivity in the subtropics is too low [Bennington et al. 2009]. Physical variability since 1948 is consistent with observations [Breeden and McKinley, 2016].

As in Breeden and McKinley [2016], the physical model was spun up for a 100 year period with 1948-1987 repeated twice and then followed again by 1948-1967, for a total physical spin up of 120 years. The biogeochemical model was then initialized using World Ocean Atlas phosphate concentrations and spun up for 10 years using 1948-1957 daily forcing. To avoid initialization shock, the model was then forced for 5 years with repeating 1948 fields before the 1948-2009 experiment started. Due Had1SSTv1.0 fields only being available through 2009, this model integration ends in 2009. Future studies using Had1SSTv1.1, which extends beyond 2009, will require re-initialization and new spin up integrations.

2.3 Phosphate diagnostics

Biogeosciences Discuss., https://doi.org/10.5194/bg-2018-89
Manuscript under review for journal Biogeosciences
Discussion started: 20 February 2018

To assess the processes modifying phosphate concentration, we employ phosphate flux diagnostics (in mmol m^{-3} yr^{-1}) for net biological processes, vertical advection and diffusion, and horizontal advection and diffusion. These terms describe the tendency of each process at every time step during the model simulation, averaged to monthly for output [Ullman et al., 2009; Breeden and McKinley, 2016]. For conciseness, the biological uptake term presented here is the sum of separate diagnostic terms for phosphate utilization by primary producers and remineralization that returns phosphate to the water column.

For analysis of mean and linear trends for 1998-2007, we use biological, vertical and horizontal diagnostic terms. Unfortunately, the biological diagnostics prior to 1998 were lost after simulations were completed. Thus, for correlations for 1949-2009, we use biomass in place of the biological diagnostics. This choice is supported by strong correlations (R=-0.87 to -0.98) between biomass and the biological diagnostics in our three focus regions (defined below) for 1998-2007. Biomass and biological diagnostics have an opposite sign because phosphate is removed as biomass accumulates.

2.4 Light and nutrient limitation

As detailed in Dutkiewicz et al. [2005], model phytoplankton growth is limited by light and the most limiting nutrient. Limiting nutrients are phosphate (PO_4) and iron (Fe) for small phytoplankton and PO_4, Fe and silicate ($SiOH_4$) for large phytoplankton. The parameterization uses Michaelis-Menton ratios that tend to 0 as the resource becomes severely limiting to growth, and approach 1 when replete. A lower value indicates a greater stress, and thus the phytoplankton group with the larger half saturation constant will be more limited for the same ambient nutrient or light concentration.

Specifically, maximum growth rates ($\mu_{max,small}$ = 1/1.3 d^{-1}, $\mu_{max,large}$ = 1/1.1 d^{-1}) are reduced through multiplication by limitation terms.

$$\mu = \mu_{max} \cdot \gamma_{light} \cdot \min\left(\gamma_{PO4}, \gamma_{Fe}, \gamma_{siOH4(large\ only)}\right) \quad (1)$$

With half saturation constants $I_{o,small}$ = 15 Wm^{-2}, $I_{o,large}$ = 12 Wm^{-2}, light limitation is:

$$\gamma_{light} = \frac{I}{I+I_o} \quad (2)$$

And for nutrients

$$\gamma_X = \frac{X}{X+K_{o,X}} \quad (3)$$

For phosphate, X = PO_4 and $K_{o,PO4,small}$ = 0.05 mmol m^{-3} and $K_{o,PO4,large}$ = 0.1 mmol m^{-3}. For iron, X = Fe and $K_{o,Fe,small}$ = 0.01 µmol m^{-3}, $K_{o,Fe,large}$ = 0.05 µmol m^{-3}. For large phytoplankton only, silicate limitation also applies, with $K_{o,SiOH4,large}$ = 2 mmol m^{-3}. Because of their higher half saturation constant for phosphate, modeled large phytoplankton are more phosphate stressed than small phytoplankton. In contrast, the higher

light half saturation makes small phytoplankton experience greater light stress. Due to high levels of aeolian dust deposition in the North Atlantic, parameterized here with the imposition of climatological fields from Mahowald et al. [2003], iron is never limiting in our study area and is not further discussed.

For this analysis, monthly mean light and nutrient fields are used to calculate limitation terms for light and nutrient for each phytoplankton type.

2.5 Analysis

Throughout the study, annual averages over the top 100 m are used. This depth is selected because it is a reasonable approximation for both the euphotic zone and the Ekman layer, and is a computationally efficient choice consistent with previous work [Long et al. 2013; Williams et al. 2000, 2014]. For analysis of light limitation, however, it is important to consider that deep mixing will move mixed layer phytoplankton to substantially below 100 m [Sverdrup, 1953]. This important effect would be poorly captured if light limitation terms were averaged only over the surface 100 m. The more appropriate choice, used here, is to use either the depth of the monthly mixed layer or 100 m, whichever is deeper. Light limitation is calculated monthly in this way and then annually averaged. For consistency, we apply the same averaging approach for nutrient limitation. However, since nutrients are homogenized by deep mixing, results for nutrient limitation are not substantially different from the use of a strict 100m average.

For physical comparisons, mixed layer depth (MLD) is calculated using monthly density fields and a criteria of 0.03 kg m^{-3} increase above the surface density. The barotropic streamfunction is calculated using a north to south integration of the full depth zonal velocity fields [Breeden and McKinley, 2016]. To find the minimum barotropic streamfunction of the subpolar gyre, the minimum within a region 60-30 ^{o}W, 50-65 ^{o}N is used. A preliminary comparison of nutrient flux variability to climate indices uses the winter (DJFM) East Atlantic Pattern (http://www.cpc.ncep.noaa.gov/data/teledoc/ea.shtml, downloaded 12.15.2017) and the winter North Atlantic Oscillation (Hurrell and NCAR, 2017).

This analysis is based on annual mean fields. A 3-month lag of the biology diagnostics and biomass fields after physical diagnostics and other physical fields is employed to account for the maximum physical forcing occurring in the winter prior to the spring bloom. Thus, annual mean physical fields are averaged from October of the prior year to September of the year in question. Biological fields are January to December averages.

To compare directly to the 10-year period of prime SeaWiFS observations, our primary focus is on linear trends over 1998-2007, with significance bounds set at $p < 0.05$ (95 %). To complement this analysis with a consideration of interannual variability across the full model experiment (1948-2009), we also consider correlations of physical and biogeochemical timeseries calculated as area-weighted averages over three selected regions (defined below), and then linearly detrended prior to correlation analysis. Because of the aforementioned biological lag, the timeframe for correlations becomes 1949-2009.

Biogeosciences Discuss., https://doi.org/10.5194/bg-2018-89
Manuscript under review for journal Biogeosciences
Discussion started: 20 February 2018

3 Results

3.1 Model comparison to observations

The simulation captures the magnitude of mean 1998-2007 subpolar biomass reasonably in comparison to the satellite-based observations (Fig. 1a, b). The detailed spatial pattern of biomass is impacted by the North Atlantic Current extension being too diffuse and too directly east-west (i.e. not turning to the northeast as it should at about 25 ºW), as is common in models of this resolution [Williams et al. 2014]. The maximum of biomass is displaced to the east. Also, subtropical biomass is too high in the Gulf Stream extension, but otherwise too low in the remainder of the basin and, thus the gradient from south to north in the model from 35-50 ºN is too sharp [Bennington et al. 2009].

Despite its imperfections, the model captures well the pattern and magnitude of statistically significant biomass trends north of 40 ºN over 1998-2007 (Fig. 1c, d). In both observations and the model, biomass declines to the east of 30 ºW from 40-50ºN and 35 ºW from 50-60ºN, while it increases to the west. For simplicity, we refer to this boundary as 30-35 ºW in our discussion. Model trends are generally weaker than the observed trends, but the coherent regions of statistically significant change are of similar size. Declines to the east occur in two regions in both model and observations, one in the northeast and one in the southeast. Consistent with the mean biomass structure, biomass trends are not in exactly the same locations as observed, but are displaced about 5º to the south in the southeast and northwest, and 5º to the south and 5º west for the northeast region.

In both observations and models, the magnitudes of these changes are large in comparison to the mean. In the declining regions, where mean biomass is 15-25 mgC m^{-3} (Fig. 1, S1), trends -0.5 to -1.5 mgC m^{-3} yr^{-1} over 10 years imply biomass reductions of 30-50 %. To the west of 30-35 ºW, increases of a comparable percentage are implied.

To focus our analysis, we select three regions in the model that capture the significant biomass changes (Fig. 1d). We will use these regions for discussion and for averaging of biogeochemical and physical terms. In the northeastern subtropical gyre, or "intergyre" [Follows and Dutkiewicz, 2002], lies our southeast (SE) region, just south of the physical separation between the subpolar and subtropical gyre based on the barotropic streamfunction (section 3.4). The SE region is bounded between 30-15 ºW and 40-50 ºN. The northeast (NE) region lies in the eastern subpolar gyre to the southeast of Iceland, 35-20 ºW and 55-60 ºN. The northwest (NW) region is south of Greenland at 35-20 ºW and 50-60 ºN.

In these three regions, annual anomalies of biomass are compared to satellite observations from SeaWiFS (1998-2007) and MODIS (2003-2015) (Fig. 2). The associated monthly biomass timeseries are presented in Fig. S1. In all regions, model anomalies are quantitatively different from the observations to a similar degree that the observations differ from each other. In the SE region, the shift from positive biomass anomalies before 2004 to negative anomalies after 2004 is found in all three timeseries, and MODIS indicates a return

Biogeosciences Discuss., https://doi.org/10.5194/bg-2018-89
Manuscript under review for journal Biogeosciences
Discussion started: 20 February 2018

to positive anomalies after 2010 (Fig. 2a). In the NE region, higher frequency variability is suggested, with mostly positive anomalies over 1998-2003 and negative anomalies from 2005-2009 (Fig. 2b). The spatial displacement between the modeled and observed anomalies (Fig. 1c, d) is not accounted for with the regions used for Fig. 2b, but these comparisons do not substantially change if the averaging region for the observations in the NE is shifted 5 degrees north and 5 degrees east (not shown). In the NW region, positive anomalies of comparable magnitude dominate 2003-2008, the timeframe over which the three records coincide (Fig. 2c). Negative anomalies are largely found both before and after. In the last 3 MODIS years, positive anomalies return to the NW region. Having demonstrated that this model reasonably captures the patterns and magnitudes of biomass change, we now use the model to explain the mechanistic drivers in all three regions over the SeaWiFS period, 1998-2007.

3.2 Nutrient changes

The model captures the mean gradients of the phosphate field well, but mean values are 10-20 % too low across most of the subpolar gyre (Fig 3a, b). Changes in the nutrient field could drive these observed and modeled changes, and as temporally resolved large-scale nutrient datasets are not available, the model alone allows us to evaluate nutrient trends (Fig 3c). Modeled nutrient concentrations decline significantly over 1998-2007 across most of the region north of 50 ^{o}N. The pattern suggests these changes are important to the declines of biomass in the SE and NE regions. However, there is no increase of phosphate in the NW region where biomass was observed to increase.

3.3 Trends of light and nutrient limitation

To better understand drivers of the biomass trends, we begin by decomposing the biomass trends into those occurring in the small and the large phytoplankton (Fig. 4). On the mean, large phytoplankton contribute more to the biomass fields in the north and west (Fig. 4a), while small phytoplankton are prevalent throughout the basin and are by far dominant in the south and east (Fig. 4b). Trends in small phytoplankton contribute most to total biomass change (Fig 1d) in the SE and NW regions, while large phytoplankton trends are more important in the NE region (Fig. 4c, d).

Phosphate limitation for large phytoplankton has a strong gradient of more limiting in the south and east to less limiting in the northwest (Fig. 5a), while light limitation for small phytoplankton has largely a south to north gradient from less to more limiting (Fig. 5b). Trends over 1998-2007 in the limitation terms illustrate that the SE and NE declines of biomass are spatially coherent with enhanced phosphate limitation (Fig. 5c), while the NW increase in biomass is spatially coherent with regions experiencing relief of light limitation (Fig. 5d). As shown in Fig. S2, mean and trends for light limitation for large phytoplankton and phosphate limitation for small phytoplankton have nearly identical patterns.

This distinction between the dominant limitations driving biomass change in the east and west is borne out with detrended interannual correlations over the full model period, 1949-2009 (Table 1). In the SE region,

phosphate limitation is strongly correlated with both small ($R_{SE\ (small,\ PO4)}$ = 0.68) and large phytoplankton ($R_{SE\ (large,\ PO4)}$ = 0.74), while light limitation is anti-correlated with biomass, i.e. less biomass occurs with more light, clearly illustrating that light is not the driving limitation. With respect to limitation terms in the NE region, the only significant correlation for large phytoplankton is to nutrient limitation ($R_{NE\ (large,\ PO4)}$ = 0.31). Thus, the large phytoplankton that quantitatively dominate the 1998-2007 biomass decline (Fig. 4d) due to nutrient limitation (Fig. 5c) also vary by a similar mechanism over the full model experiment.

In the NW region, the 1998-2007 biomass trend is dominated by small phytoplankton (Fig. 4d) via light limitation (Fig. 5d), and these relationships also hold for the full model experiment. Small phytoplankton light limitation is positively correlated with small phytoplankton biomass ($R_{NW(small,light)}$ = 0.61), while small phytoplankton biomass is reduced when more phosphate is available ($R_{NW(small,PO4)}$ = -0.50, Table 1). Though large phytoplankton have the opposite sensitivities ($R_{NW(large,light)}$ = -0.63, $R_{NW(large,PO4)}$ = 0.83), they are only 40 % of the total biomass (not shown) and have a lesser role in total biomass changes (Fig. 4c).

In the model, silicate is also limiting to large phytoplankton and its limitation also becomes more intense over 1998-2007 to the north of 50 °N (Fig. S2f). However, variability in silicate limitation is highly correlated to variability of phosphate limitation in the NW and NE areas for 1949-2009 ($R_{NE(PO4,SiOH4)}$ = 0.91, $R_{NW(PO4,SiOH4)}$ = 0.83, Table S1). Due to these high correlations and the fact that large phytoplankton are only dominant to biomass trends in the NE region (Fig. 4c), the remaining analysis addresses only phosphate fluxes. For completeness, 1998-2007 light and silicate limitation trends for large phytoplankton and phosphate limitation for small phytoplankton are shown in Fig. S2, and 1949-2009 correlations in the three regions are given Table S1.

3.4 Physical changes and their impacts on light and nutrient limitation

There are significant physical changes in the subpolar gyre that influence the nutrient and light fields. The model barotropic streamfunction experiences a positive change from a minimum value of -41 Sv for 1998-2000 to -28 Sv for 2005-2007 (Fig. 6). With this anomaly, the zero line of the streamfunction shifts several degrees north at 45-40 °W and more modestly to the north in the east (bold black contours in Fig. 6a and Fig. 6b). The North Atlantic Current (NAC) flows along this contour, indicating a northward shift of the NAC.

Consistent with the weakening of the subpolar gyre, mixed layers shoal substantially, particularly to the west of 30-35 °W (Fig. 7a, b). A dramatic shoaling of maximum mixed layers is found in the NW region, going from almost 1200 m to less than 400 m (Fig. 7e). This shoaling explains the strong decline in light limitation in the NW region. There is modest shoaling of mixed layers in the NE region (Fig. 7d) and there is no significant trend in the SE region (Fig. 7c). Shoaling in the NE could contribute to the reduction in phosphate availability and reduced biomass. However, the lack of mixed layer depth change in the SE suggests that less vertical mixing is not the dominant driver of reduced biomass here.

3.5 Phosphate diagnostics

Biogeosciences Discuss., https://doi.org/10.5194/bg-2018-89
Manuscript under review for journal Biogeosciences
Discussion started: 20 February 2018

To fully assess the three-dimensional physical drivers of phosphate supply to the NE and SE regions, we employ phosphate diagnostics. On the mean for 1998-2007 across the northern North Atlantic, vertical advection and diffusion supplies phosphate to the euphotic zone (Fig. 8a), with the supply being much stronger in the region of deepest mixed layers (Fig. 7). Horizontal advection and diffusion strongly diverges the converging vertical flux (Fig. 8b), leading to strong negative fluxes (divergence) coincident with strongly positive vertical fluxes. The horizontal divergence centered at about 30-35 °W leads to positive horizontal fluxes (convergence) to the east and also to the west south of 50 °N. As the sum of the vertical and horizontal components is net positive (Fig. 8c), the mean three-dimensional advection and diffusion net supplies phosphate to the subpolar gyre. The pattern of this supply is strongly influenced by both vertical and horizontal processes. Biological processes remove the physically-supplied phosphate from the surface ocean (Fig. 8d).

To east of 30-35 °W, horizontal and vertical phosphate fluxes are comparable in magnitude and both supply nutrients to the surface (Fig. 8, 9). In the SE region, mean 1998-2007 vertical advection and diffusion supplies 0.13 mmol m^{-3} yr^{-1} while horizontal supplies 0.07 mmol m^{-3} yr^{-1}, together supporting biological utilization of -0.20 mmol m^{-3} yr^{-1} (Fig. 9a). In the NE region, the mean vertical supply is 0.24 mmol m^{-3} yr^{-1} while horizontal supplies 0.08 mmol m^{-3} yr^{-1}, and thus a mean biological utilization of -0.32 mmol m^{-3} $yr^{-1}$is supported (Fig. 9b). The collaborative supply of vertical and horizontal fluxes in these regions can be contrasted to the NW region where the mean vertical supply is 0.33 mmol m^{-3} yr^{-1}, and from this the horizontal divergence removes about 25 % (-0.08 mmol m^{-3} yr^{-1}) and biology removes the remainder (-0.24 mmol m^{-3} yr^{-1}, Fig. 9c). In all three regions, variability in both horizontal and vertical fluxes is quantitatively similar to the biological flux variability (Fig. 9).

For 1998-2007, trends in the supply and removal of phosphate indicate a large decrease in supply via vertical fluxes to the west of 30-35 °W (Fig. 10a) and a corresponding strong reduction in the horizontal divergence of phosphate, a positive anomaly (Fig 10b, 9c). To the west of 30-35 °W, these opposing trends of the vertical and horizontal fluxes largely negate each other. However, to the east of 30-35 °W there are weak and mostly negative tendencies in the vertical and significant negative trends in the horizontal terms. Thus, the net physical phosphate supply in the eastern subpolar gyre has an overall negative trend, albeit only large enough to be formally statistically significant in parts of the SE region (Fig. 9c). The pattern of reduced phosphate supply is consistent with the pattern of significant reduction in biomass (Fig. 1d) and significant positive tendencies in the biological diagnostic (Fig. 10d). In summary, the model indicates that from 1997 to 2008, reduced vertical supply of nutrients to the west of 30-35 °W led to less horizontal convergence of nutrients to the east of 30-35 °W, and thus less phosphate available for biological production. This mechanism can explain the SeaWiFS-observed declines in biomass in the eastern subpolar gyre and northeastern subtropical gyre over this period.

Long-term (1949-2009) correlations between physical diagnostic terms and biomass support the conclusion that variability in horizontal fluxes are important to biomass interannual variability to the east of 30-35 °W

Biogeosciences Discuss., https://doi.org/10.5194/bg-2018-89
Manuscript under review for journal Biogeosciences
Discussion started: 20 February 2018

(Table 2). In both the SE and NE region, horizontal fluxes are significantly correlated to biomass ($R_{SE(Biomass,Horiz)}$ = 0.44, $R_{NE(Biomass,Horiz)}$ = 0.48), suggesting that the 1998-2007 relationships are indicative of interannual behavior over the long-term, wherein reduced horizontal nutrient supply leads to reduced biomass. For the SE region on the long term, vertical fluxes have also a significant correlation ($R_{SE(Biomass,Vert)}$ = 0.63), indicating that longer term interannual change in biomass in this region is determined by variability in both horizontal and vertical fluxes. In the NW region, biomass and horizontal fluxes are also positively correlated ($R_{NW(Biomass,Horiz)}$ = 0.69), but this appears to be an indirect relationship. As light limitation is relieved, biomass increases, and at the same time vertical convergence of phosphate is reduced (Fig 10a) and there is a positive anomaly in the horizontal divergence (Fig. 10b). Consistent with this interpretation, vertical and horizontal convergence are strongly anti-correlated in the NW region ($R_{NW(Horiz,Vert)}$ = -0.76).

The impact of the physical drivers discussed earlier in this section on 1949-2009 biomass variability varies by study region. For the SE region, where biomass is positively driven by both horizontal and vertical nutrient fluxes, biomass declines with positive anomalies of the minimum barotropic streamfunction of the subpolar gyre ($R_{SE(Biomass,PsiMin)}$ = -0.37, Table 2), consistent with 1997-2008 relationships. However, the minimum barotropic streamfunction is not itself correlated to either horizontal or vertical fluxes. Vertical supply is not a significant driver for 1997 to 2008 changes, but for the longer term, vertical nutrient fluxes decrease with shallower mixed layers (a negative anomaly) and warmer temperatures ($R_{SE(MLD,Vert)}$ = 0.66, $R_{SE(SST,Vert)}$ = -0.64).

For both the NE and NW regions, correlations between changing minimum barotropic streamfunction (Fig. 6), shoaling mixed layers (Fig. 7) and horizontal and vertical nutrient supply (Fig. 10) for 1949-2009 are generally weak and, in fact, opposite in sign to the relationships for the SeaWiFS period. For 1998-2007, the minimum barotropic streamfunction experienced a positive anomaly, mixed layers shoaled, and horizontal fluxes declined in the NE region. For 1949-2009, positive anomalies of the minimum barotropic streamfunction are, instead, weakly associated with increased horizontal nutrient fluxes ($R_{NE(PsiMin,Horiz)}$ = 0.25). At the same time, shallower mixed layers (a negative anomaly) are associated with decreased vertical fluxes and increased horizontal fluxes ($R_{NE(MLD,Vert)}$ = 0.52, $R_{NE(MLD,Horiz)}$ = -0.42). In the NW region, light limitation is clearly the driver of biomass changes on both timescales (Fig. 1,4, Table 1), but large negative anomalies of vertical fluxes and positive anomalies of horizontal fluxes also occur as mixed layers shoal over 1997-2008 (Fig. 9, 10). However, for 1949-2009 in the NW, the reverse is found; vertical fluxes increase and horizontal nutrient fluxes decrease coincident with shallower mixed layers ($R_{NW(MLD,Vert)}$ = -0.33, $R_{NW(MLD,Horiz)}$ = 0.46). Long-term correlations of physical changes to nutrient fluxes in the two subpolar regions differ from those occurring with 1998-2007 trends is consistent with the weak long-term correlations that explain no more than 30% of the variance. The lack of consistent associations between biomass and physical variability over both timescales illustrates the complexity of the system and makes clear that relationships revealed by relatively short-lived observing systems are not necessarily representative of the long term.

Biogeosciences Discuss., https://doi.org/10.5194/bg-2018-89
Manuscript under review for journal Biogeosciences
Discussion started: 20 February 2018

4 Discussion

The decline in the strength of the subpolar gyre modeled here (Fig. 6) is consistent with observations in the North Atlantic in since the mid-1990s [Häkkinen and Rhines, 2004; Hátún et al., 2005; Foukal and Lozier, 2017]. We show here that these physical changes have substantial impacts on the light field and the redistribution of nutrients in the vertical and the horizontal, and that these changes are sufficient to explain satellite-observed biomass trends over 1998-2007. Foukal and Lozier [2017] provide an updated analysis with respect to the relationship of physical changes in the gyre to the East Atlantic Pattern (EA) and the North Atlantic Oscillation (NAO). While the EA indicates the position of the westerly winds, NAO indicates their strength [Foukal and Lozier, 2017; Comas-Bru and McDermott, 2014]. A preliminary investigation using the winter (DJFM) EA index from NOAA CPC indicates that only in the nutrient-limited SE region are there significant correlations. Biomass is correlated to the EA ($R_{SE(EA,Biomass)}$ = 0.48), a relationship apparently driven by horizontal fluxes ($R_{SE(EA,Horiz)}$ = 0.43). In the SE region, biomass is not significantly correlated to the winter (DJFM) NAO [Hurrell and NCAR, 2017], which may be due to significant opposing impacts of the NAO on horizontal and vertical nutrient fluxes ($R_{SE(NAO,\ Horiz)}$ = 0.37, $R_{SE(NAO,\ Vert)}$ = -0.30). These correlations are all zero-lag. We do not find stronger correlations when biomass lags the EA or NAO by up to 3 years. That there are no significant correlations north of 50 ºN, in the NE and NW regions, between these climate modes and biomass is consistent with the weak correlations of horizontal and vertical fluxes to physical fields (Table 2).

Williams and Follows [1998] illustrate that on the mean, horizontal Ekman fluxes in the surface are critical to nutrient supply in the North Atlantic from 40-60 ºN, particularly for the northeast subtropical gyre. Yet, Williams et al. [2000] find Ekman nitrate flux variability to be an order of magnitude smaller than convective flux variability in this region. We find that 0-100 m horizontal nutrient convergence contributes 25-35 % of the mean nutrient supply in our two regions to the east of 35 ºW. In contrast to Williams et al. [2000], we do find horizontal fluxes to be important to variability, with the 1949-2009 standard deviation of horizontal fluxes in the SE region being 66 % of the standard deviation of the sum of vertical and horizontal fluxes, while the vertical flux standard deviation is 95 % of the sum. In the NE region, vertical and horizontal fluxes are anti-correlated ($R_{NE(Vert,Horiz)}$ = -0.64, Table 2) such that their variability partially cancels. The standard deviation of vertical fluxes here is 125 % of the sum, while the standard deviation of horizontal fluxes is 108 % of the sum. These very different findings can at least be partially attributed to the fact that Williams et al. [2000] had only a climatological nitrate data field to couple to their mixed layer model and windstress-based Ekman divergence calculation. The use of smooth climatological nutrient field would not likely allow for the strong co-variance between vertical and horizontal supply terms that the run-time diagnostics used here are able to reveal. As variability of nutrient supply to the surface ocean is critical to subpolar North Atlantic biomass variability, datasets that temporally resolve upper ocean nutrient fields would be most valuable to future studies. Large-scale deployment of autonomous floats with biogeochemical sensors will be essential to the development of these critical datasets [Johnson et al. 2009].

We find that reduced horizontal nutrient supply over the SeaWiFS period (1998-2007) drove the observed reductions in biomass on the northeastern flank of the North Atlantic subtropical gyre (our SE region). This mechanism contrasts to previous analyses that attributed the observed changes to increased stratification and the associated reduced vertical supply of nutrients [Behrenfeld et al. 2006; Polovina et al. 2008; Martinez et al. 2009]. Though for 1949-2009 in our SE region, we do find anti-correlation between biomass and SST ($R_{SE(Biomass, SST)}$ = -0.57, Table 2) and correlation of biomass anomalies to both vertical and horizontal nutrient supply changes ($R_{SE(Biomass,Vert)}$ = 0.63, $R_{SE(Biomass,Horiz)}$ = 0.44), it is clear that over the SeaWiFS period, reduced horizontal fluxes drive biomass declines (Fig. 10). SST as a proxy for stratification is alone insufficient to describe biomass changes in this region, and it is reasonable to expect the same the edges of the subtropical gyres elsewhere around the globe. Instead, a three-dimensional perspective on nutrient supply should be taken when observations are interpreted and when the expected mechanisms of future change are considered [Doney 2006; Bopp et al. 2013].

North Atlantic biomass variability to the north of 40 ^{o}N is quite heterogeneous and dependent on different mechanisms at distinct locations and the dominant mechanisms shift across timescales. Though a large-scale averaging approach may be appropriate for some biogeochemical studies [Fay and McKinley, 2013, 2014], relationships between the surface ocean carbon cycle and productivity may not be well captured by correlations over large-scale ocean biomes that take the whole of the subpolar gyre as one region [Fay and McKinley, 2017]. A more granular approach will likely support a deeper understanding of biological coupling to the carbon cycle this region.

These findings suggest myriad directions for further analysis. This analysis does not elucidate how variability in physical supply of silicate impacts biomass variability. Particularly considering long-term correlations between physical drivers and phosphate supply in NE and NW region that are opposite to those evidenced for 1998-2007, a complementary analysis of variability in silicate supply may be useful. Similarly, it would be of value to study the relative impacts of large and small phytoplankton size classes on total biomass variability particularly northwest region where light and nutrient limitation drive biomass in opposite directions (Table 1). Assessment of the modulation of subsurface nutrient fields by subpolar gyre physical changes, and in turn how these subsurface changes influence surface biomass would be worthwhile. Spatial analysis based on empirical orthogonal functions [Breeden and McKinley, 2016] could illustrate the dominant large-scale modes of biomass variability and may reveal the degree to which climate modes impact biomass. With respect to the period of satellite observations, a numerical simulation that covers both the SeaWiFS and MODIS period would allow study of the period since 2007 in which 1998-2007 trends appear to largely have reversed (Fig. 2). For such a simulation, greater physical resolution should improve representation of the gyre structure and its variability. Though the current ecosystem is able to capture the large-scale patterns of biomass change remarkably well, it would also be value to assess the impact of different levels of ecosystem complexity in future modeling work.

5 Conclusions

In the North Atlantic from 40-60 ºN over 1998-2007, biomass estimated from SeaWiFS ocean color increases to the west of 30-35 ºW and declines to the east. A regional coupled physical-biogeochemical model that reproduces 1998-2007 trends indicates that the relief of light limitation with shoaling mixed layers drives the observed biomass increase in the west. Biomass declines to the east of 30-35 ºW over 1998-2007 are due to reduced nutrient supply. On the northeastern flank of subtropical gyre, in our southeast region, changing horizontal nutrient supply drives biomass change over the SeaWiFS period. For the full model experiment, 1949-2009, both horizontal and vertical nutrient supply are important to interannual variability in here. In the northeast subpolar gyre, horizontal nutrient supply is the most important driver of biomass variability both for the 1998-2007 SeaWiFS period and for the full model experiment.

Though nutrient supply in three dimensions is clearly driving biomass changes to the east of 30-35 ºW, clear connections between supply terms and large-scale physics or climate indices are elusive. Neither does the minimum of the barotropic streamfunction of the subpolar gyre or local mixed layer depth change consistently explain nutrient flux changes both for the satellite observed period and the full model experiment. In the southeast, biomass variability over 1949-2009 weakly correlates to the East Atlantic (EA) pattern, but nowhere does the NAO explain biomass variability. Given the evidence here that horizontal and vertical nutrient supply are important to biomass variability, and evidence from other studies that these modes of climate influence the gyre strength, currents, deep mixing, and Ekman suction and divergence of the subpolar gyre, more investigation of the links between North Atlantic climate and biomass variability is clearly warranted.

Acknowledgments

The authors thank Val Bennington, Lucas Gloege, Dierk Polzin, Melissa Breeden, and Amanda Fay for their assistance with the model and datasets. We gratefully acknowledge funding from NASA (NNX/11AF53G, NNX/13AC53G, NNX13AC94G). We thank the Oregon State Ocean Productivity group for providing biomass data.

Biogeosciences Discuss., https://doi.org/10.5194/bg-2018-89
Manuscript under review for journal Biogeosciences
Discussion started: 20 February 2018

References

Antonov, J. I., Locarnini, R.A., Boyer, T.P., Mishonov, A.V., and Garcia, H.E.: World Ocean Atlas 2005, vol. 2, Salinity, NOAA Atlas NESDIS 62, edited by: Levitus, S., US Govt. Print. Off., Washington, D. C., 182 pp. 2006.

Behrenfeld, M., O'Malley, R., Siegel, D., McClain, C., Sarmiento, J., Feldman, G., Milligan, A.J., Falkowski, P.G., Letelier, R.M., and Boss, E.S.: Climate-driven trends in contemporary ocean productivity, Nature, 444, 752-755. 2006.

Bennington, V., McKinley, G. A. , Dutkiewicz, S. and Ullman, D.: What does chlorophyll variability tell us about export and CO_2 flux variability in the North Atlantic?, Global Biogeochem. Cycles, 23, GB3002, doi:10.1029/2008GB003241, 2009.

Bopp, L., Resplandy L., Orr, J.C., Doney, S.C., Dunne, J.P., Gehlen, M., Halloran, P. Heinze, C., Ilyina, T., Séférian, R., Tjiputra, J. and Vichi, M.: Multiple stressors of ocean ecosystems in the 21st century: projections with CMIP5 models. Biogeosciences 10, 6225–6245, 2013.

Breeden, M. L. and McKinley, G.A.: Climate impacts on multidecadal pCO_2 variability in the North Atlantic: 1948–2009. Biogeosciences 13, 3387–3396, 2016.

Comas-Bru, L., and McDermott, F.: Impacts of the EA and SCA patterns on the European twentieth century NAO-winter climate relationship, Q. J. R. Meteorol. Soc., 140, 354–363,2014.

Dave, A. C. and Lozier, M.S.: Local stratification control of marine productivity in the subtropical North Pacific, J. Geophys. Res., 115, C12032, doi:10.1029/2010JC006507, 2010.

Dave, A. C. and Lozier, M. S. Examining the global record of interannual variability in stratification and marine productivity in the low-latitude and mid-latitude ocean. J Geophys Res-Oceans 118, 3114–3127, doi: 10.1002/jgrc.20224, 2013.

Dave, A. C. and Lozier, M.S.: The Impact of Advection on Stratification and Chlorophyll Variability in the Equatorial Pacific. Geophys Res Lett. doi:10.1002/2015GL063290, 2015.

Dave, A. C., Barton, A.D., Lozier, M.S., and McKinley, G.A.: What drives seasonal change in oligotrophic area in the subtropical North Atlantic?, J. Geophys. Res. Oceans, 120, doi:10.1002/ 2015JC010787, 2015.

Doney, S.C.: Plankton in a warmer world, Nature, 444, 695-696, 2006.

Dutkiewicz, S., Follows, M.J., Marshall, J., and Gregg, W.W.: Interannual variability of phytoplankton abundances in the North Atlantic, Deep-Sea Res. II, 48, 2323-2344, 2001.

Dutkiewicz, S., Follows, M.J.,, and Parekh, P.: Interactions of the iron and phosphorus cycles: A three-dimensional model study, Global Biogeochem. Cycles, 19, GB1021, doi:10.1029/2004GB002342, 2005.

Fay, A.R. and McKinley G.A.: Global trends in surface ocean pCO2 from in situ data. Global Biogeochem Cycles 27, 1–17, 2013.

Fay, A.R. and McKinley G.A.: Global open-ocean biomes: mean and temporal variability. Earth Syst. Sci. Data 6, 273–284, 2014.

Fay, A.R. and McKinley G.A.: Correlations of surface ocean pCO2 to satellite chlorophyll on monthly to interannual timescales. Global Biogeochem Cycles 31, 436–455, 2017.

Follows, M.J. and Dutkiewicz, S.: Meteorological modulation of the North Atlantic spring bloom, Deep Sea Res. II, 49, 321-344, 2002.

Foukal, N. P. and Lozier, M. S. Assessing variability in the size and strength of the North Atlantic subpolar gyre. J Geophys Res-Oceans 122, 6295–6308, 2017.

Fox-Kemper, B., Ferrari, R. and Hallberg, R. W.: Parameterization of mixed layer eddies. Part I: Theory and diagnosis. Journal of Physical Oceanog. 38, 1145–1165, 2008.

Garcia, H. E., Locarnini, R.A., Boyer, T.P., and Antonov, J.I.: World Ocean Atlas 2005, vol. 4, Nutrients (Phosphate, Nitrate, Silicate), NOAA Atlas NESDIS 64, edited by S. Levitus, 396 pp., U.S. Govt. Print. Off., Washington, D. C., 2006.

Gent, P. R. and McWilliams, J.C.: Isopycnal mixing in ocean circulation models, J. Phys. Oceanogr., 20, 150-155, 1990.

Häkkinen, S. and Rhines, P.B.: Decline of the subpolar North Atlantic circulation during the 1990s, Science, 304, 555-559, 2004.

Hátún, H., Sandø, A.B., Drange, H., Hansen, B. and Valdimarsson, H.: Influence of the Atlantic subpolar gyre on the thermohaline circulation, Science, 309, 1841-1844, 2005.

Hátún, H., Lohmann K., Matei D., Jungclaus J., Pacariz S., Bersch M., Gislason A., Olafsson J., and Reid R.C : An inflated subpolar gyre blows life toward the northeastern Atlantic. Progress in Oceanography 147, 49–66, 2016.

Hátún, H. Azetsu-Scott K., Somavilla R., Rey F., Johnson C., Mathis M., Mikolajewicz U., Coupel P., Tremblay J., Hartman S., Pacariz S.V., Salter I., and Olafsson J.: The subpolar gyre regulates silicate concentrations in the North Atlantic. Scientific Reports 14576, doi:10.1038/s41598-017-14837-4, 2017.

Hurrell, J. and NCAR (eds): The Climate Data Guide: Hurrell North Atlantic Oscillation (NAO) index (station based), 2017. Retrieved from https://climatedataguide.ucar.edu/climate-data/hurrell-north-atlantic-oscillation-nao-index-station-based. Last modified 07 Nov 2017.

Johnson, K. S.,. Berelson, W. M,. Boss, E.S., Chase, Z., Claustre, H., Emerson, S.R., Gruber, N., Koertzinger, A., Perry, M.J., and Riser, S.C.: Observing biogeochemical cycles at global scales with profiling floats and gliders prospects for a global array, Oceanography, 22(3), 216–225, doi:10.5670/oceanog.2009.81, 2009.

Johnson, C., Inall, M. and Häkkinen, S.: Declining nutrient concentrations in the northeast Atlantic as a result of a weakening Subpolar Gyre. Deep-Sea Research Part I 82, 95–107, 2013.

Kalnay, E., Kanamitsu, M., Kistler, R., Collins, W., Deaven, D., Gandin, L., Iredell, M., Saha, S., White, G., Woollen, J., Zhu, Y., Leetmaa, A., and Reynolds, R.: The NCAR/NECP 40-year reanalysis project, Bull. Amer. Meteor. Soc., 77, 437-471, 1996.

Koch, J., McKinley, G. A., Bennington, V. and Ullman, D.: Do hurricanes cause significant interannual variability in the air ‐ sea CO2 flux of the subtropical North Atlantic? Geophys Res Lett 36, L07606, 2009.

Large, W. G., McWilliams, J.C., and Doney, S.C.: Oceanic vertical mixing: A review and a model with a nonlocal boundary layer parameterization, Rev. Geophys., 32, 363-403, 1994.

Lozier, M. S., Leadbetter, S., Williams, R.G., Roussenov, V., Reed, M.S.C., and Moore, N.J.: The spatial pattern and mechanisms of heat-content change in the North Atlantic, Science, 319, 800-803, 2008.

Lozier, M.S., Dave, A.C., Palter, J.B., Gerber, L.M., and Barber, R.T.: On the relationship between stratification and primary productivity in the North Atlantic, Geophys. Res. Lett., 38, L18609, doi:10.1029/2011GL049414., 2011.

Mahowald, N., Lou, C., del Corral, J., and. Zender, C.: Interannual variability in atmospheric mineral aerosols from a 22-year model simulation and observational data, J. Geophys. Res., 108(D12), 4352, doi:10.1029/2002JD002821, 2003.

Marshall, J. C., Adcroft, A., Hill, C., Perelman, L., and Heisey, C.: A finite volume, incompressible Navier-Stokes model for studies of the ocean on parallel computers, J. Geophys. Res., 102, 5753-5766, 1997a.

Marshall, J.C., Hill, C., Perelman, L., and Adcroft, A.: Hydrostatic, quasi-hydrstatic and non-hydrostatic ocean modeling, J. Geophys. Res., 102, 5733-5752, 1997b.

Martinez, E., Antoine, D., D'Ortenzio, F., and Gentili, B.: Climate-driven basin-scale decadal oscillations of oceanic phytoplankton, Science, 326, 1253-1256, 2009.

McClain, C.R., Feldman, G.C., and. Hooker, S.B.: An overview of the SeaWiFS project and strategies for producing a climate research quality global ocean bio-optical time series, Deep Sea Res. II, 51, 5-42, 2004.

McGillicuddy, D.J., Jr., Anderson, L.A.,Doney, S.C., and Maltrud, M.E.: Eddy-driven sources and sinks of nutrients in the upper ocean: Results from a 0.1° resolution model of the North Atlantic, Global Biogeochem. Cycles, 17, 1035, doi:10.1029/2002GB001987 2, 2003.

Oschlies, A.: Nutrient supply to the surface waters of the North Atlantic: A model study, J. Geophys. Res., 107, doi:10.1029/2000JC000275, 2002.

Palter, J. B., Lozier, M. S., and Barber, R.T.: The effect of advection on the nutrient reservoir in the North Atlantic subtropical gyre, Nature, 437, 687-692, 2005.

Pelegrí, J. L., Csanady, G.T., and Martins, A.: The North Atlantic nutrient stream, J. Oceanogr., 52, 275-299, 1996.

Polovina, J. J., Howell, E.A., and Abecassis, M.; Ocean's least productive waters are expanding, Geophys. Res. Lett., 35, L03618, doi:10.1029/2007GL031745, 2008.

Rayner, N. A., Parker, D. E., Horton, E. B., Folland, C. K., Alexander, L. V., Rowell, D. P., Kent, E. C., and Kaplan, A.: Global analyses of sea surface temperature, sea ice, and night marine air temperature since the late nineteenth century, J. Geophys. Res., 108, 4407, doi:10.1029/2002JD002670, 2003.

Siegel, D.A., Doney, S.C., and Yoder, J.A.: The North Atlantic spring phytoplankton bloom and Sverdrup's critical depth hypothesis, Science, 296, 730-733, 2002.

Siegel, D.A., Maritorena, S., Nelson, N.B., and Behrenfeld, M.J.: Independence and interdependencies among global ocean color properties: Reassessing the bio-optical assumption, J. Geophys. Res.,110, C07011, doi:10.1029/2004JC002527, 2005.

Sverdrup, H. U.: On conditions for the vernal bloom of phytoplankton, J. Cons. Perm. Int. Explor. Mer., 18, 287-295, 1953.

Ullman, D.J., McKinley, G.A.,Bennington, V., and Dutkiewicz, S.: Trends in the North Atlantic carbon sink: 1992-2006, Global Biogeochem. Cycles, 23, GB4011, doi:10.1029/2008GB003383, 2009.

Westberry, T., Behrenfeld, M.J., Siegel, D.A., and Boss, E.S.: Carbon-based primary productivity modeling with vertically resolved photoacclimation. Global Biogeochem. Cycles, 22, GB2024, doi:10.1029/2007GB003078, 2008.

Williams, R.G. and Follows, M.J.: The Ekman transfer of nutrients and maintenance of new production over the North Atlantic, Deep-Sea Res. I, 45, 461-489, 1998.

Williams, R.G., McLaren, A.J. and Follows, M.J.: Estimating the convective supply of nitrate and implied variability in export production over the North Atlantic. Global Biogeochem Cy 14, 1299–1313, 2000.

585 Williams, R.G., Roussenov, V. and Follows, M. J.: Nutrient streams and their induction into the mixed layer, Global Biogeochem. Cycles, 20, GB1016, doi:10.1029/2005GB002586, 2006.

Williams, R.G., Roussenov, V., Smith, D. and Lozier, M.S.: Decadal Evolution of Ocean Thermal Anomalies in the North Atlantic: The Effects of Ekman, Overturning, and Horizontal Transport. Journal of Climate 27, 698–719, 2014.

590 Yoder, J.A. and. Kennelly, M.A.: Seasonal and ENSO variability in global ocean phytoplankton chlorophyll derived from 4 years of SeaWiFS measurements, Global Biogeochem. Cycles, 17, 1112, doi:10.1029/2002GB001942, 2003.

Biogeosciences Discuss., https://doi.org/10.5194/bg-2018-89
Manuscript under review for journal Biogeosciences
Discussion started: 20 February 2018

Tables

Table 1: Correlations of phosphate and light limitation for small phytoplankton to large and small biomass, 1949-2009. For conciseness, shown here are only small phytoplankton limitation terms, but since these are ratios calculated from identical fields, the correlations are very similar large phytoplankton (Table S1). Bold indicates statistical significance ($p < 0.05$). Detrending is applied prior to correlation analysis.

SOUTHEAST	large biomass	phosphate limitation, small phytoplankton	light limitation, small phytoplankton
small biomass	**0.52**	**0.68**	**-0.75**
large biomass	-	**0.74**	**-0.57**
phosphate limitation, small		-	**-0.87**

NORTHEAST	large biomass	phosphate limitation, small phytoplankton	light limitation, small phytoplankton
small biomass	**0.36**	-0.09	-0.08
large biomass	-	**0.31**	-0.17
phosphate limitation, small		-	**-0.87**

NORTHWEST	large biomass	phosphate limitation, small phytoplankton	light limitation, small phytoplankton
small biomass	**-0.34**	**-0.50**	**0.61**
large biomass	-	**0.83**	**-0.63**
phosphate limitation, small		-	**-0.71**

Biogeosciences Discuss., https://doi.org/10.5194/bg-2018-89
Manuscript under review for journal Biogeosciences
Discussion started: 20 February 2018

Table 2: Correlations of biomass to physical drivers and horizontal and vertical phosphate diagnostics, 1949-2009. The minimum barotropic streamfunction is found within 60-30 ºW, 50-65 ºN; maximum mixed layer depth (MLD) and sea surface temperature (SST) are area-weighted averages for each of the three averaging regions. Bold indicates statistical significance ($p < 0.05$). Detrending is applied prior to correlation analysis.

SOUTHEAST	Minimum Barotropic Streamfunction	Maximum MLD	SST	Horizontal	Vertical
Biomass	**-0.37**	**0.54**	**-0.57**	**0.44**	**0.63**
Minimum Barotropic Streamfunction	-	**-0.42**	**0.38**	-0.18	-0.23
Maximum MLD		-	**-0.65**	0. 10	**0.66**
SST			-	-0.02	**-0.64**
Horizontal				-	**-0.29**

NORTHEAST	Minimum Barotropic Streamfunction	Maximum MLD	SST	Horizontal	Vertical
Biomass	0.18	-0.02	0.08	**0.48**	-0.25
Minimum Barotropic Streamfunction	-	**-0.60**	**0.72**	**0.25**	-0.22
Maximum MLD		-	**-0.76**	**-0.42**	**0.52**
SST			-	**0.34**	**-0.28**
Horizontal				-	**-0.64**

NORTHWEST	Minimum Barotropic Streamfunction	Maximum MLD	SST	Horizontal	Vertical
Biomass	0.14	**0.28**	-0.23	**0.69**	**-0.42**
Minimum Barotropic Streamfunction	-	**-0.42**	**0.67**	0.08	-0.10
Maximum MLD		-	**-0.42**	**0.46**	**-0.33**
SST			-	**-0.52**	**0.43**
Horizontal				-	**-0.76**

Figures

Figure 1: Surface ocean biomass (a) estimated from SeaWiFS using the CbPM model, (b) 0-100m modeled biomass, (c) SeaWiFS trend 1998-2007, and (d) 0-100m modeled biomass trend 1998-2007. In c and d, significant trends are marked with a black contour. In d, the three focus regions are outlined in red.

Figure 2: Annual anomalies of surface ocean biomass for SeaWiFS (1998-2007, red), MODIS (2003-2015, blue) and model (1998-2009, 0-100m, black) (a) SE region, (b) NE region, and (c) NW region. The corresponding monthly timeseries is shown in Fig. S1.

Figure 3: Phosphate (a) World Ocean Atlas (Garcia et al. 2006) (b) 0-100m modeled phosphate, (c) 0-100m modeled phosphate tred 1998-2007. In c, significant trends are marked with a black contour and the three focus regions are outlined in red.

Figure 4: Surface ocean small and large phytoplankton biomass (a) 0-100m modeled small phytoplankton biomass, (b) 0-100m modeled large phytoplankton biomass, (c) small phytoplankton trend 1998-2007, and (d) large phytoplankton trend 1998-2007. In c and d, significant trends are marked with a black contour and the three focus regions are outlined in red.

Figure 5: Terms for limitation by (a) phosphate, large phytoplankton (Eq. 3) (b) Light, small phytoplankton (Eq. 2), (c) 1998-2007 trend in phosphate limitation, and (d) 1998-2007 trend in light limitation. All are unitless. In c and d, significant trends are marked with a black contour and the three focus regions are outlined in red.

Figure 6: Barotropic streamfunction (a) 1998-2000 mean and (b) 2005-2007 mean. The zero streamfunction contours between 55-15°W for each period (bold black) and for the 1998-2007 mean (white) are marked.

Figure 7: Maximum mixed layer depths for (a) 1998-2000 mean and (b) 2005-2007 mean. Timeseries of monthly mixed layers for (c) SE region, (d) NE region, and (e) NW region.

Figure 8: Phosphate diagnostics, 0-100m (mmol m^{-3} yr^{-1}) for (a) vertical flux, (b) horizontal, (c) net physical, and (d) biological. Biological is negative because biomass removes phosphate from the surface ocean. The three focus regions are outlined in red in each panel.

Figure 9: Phosphate diagnostics 1998-2007 annual timeseries, 0-100m (mmol m^{-3} yr^{-1}) for (a) SE region, (b) NE region, and (c) NW region.

Figure 10: Phosphate diagnostics 1998-2007 trends, 0-100m (mmol m^{-3} yr^{-2}) for (a) vertical flux, (b) horizontal, (c) net physical, and (d) biological. Positive biological trends are consistent with negative biomass trends because less phosphate is removed as less biomass is formed. Significant trends are marked with a black contour and the three focus regions are outlined in red in each panel.

Biogeosciences Discuss., https://doi.org/10.5194/bg-2018-89
Manuscript under review for journal Biogeosciences
Discussion started: 20 February 2018

Figure 1

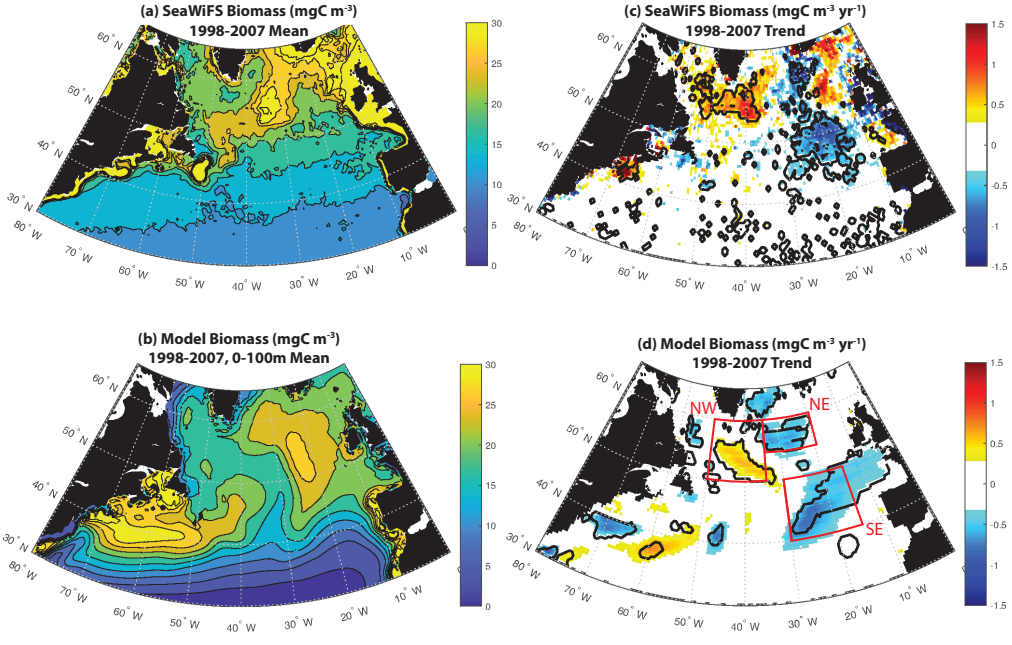

Biogeosciences Discuss., https://doi.org/10.5194/bg-2018-89
Manuscript under review for journal Biogeosciences
Discussion started: 20 February 2018

Figure 2

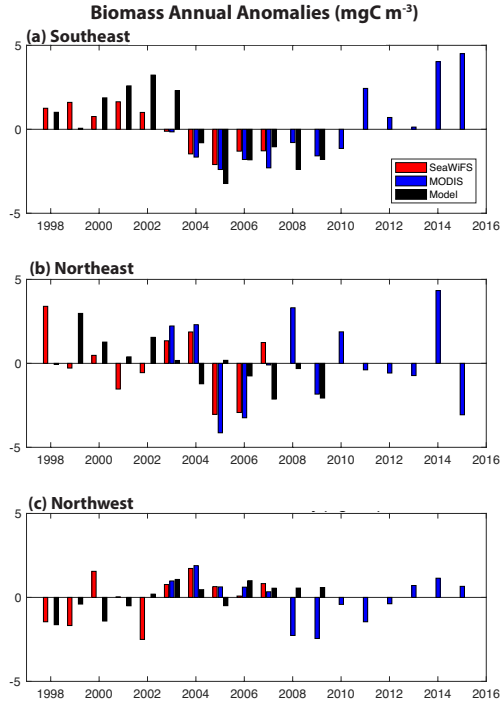

Biogeosciences Discuss., https://doi.org/10.5194/bg-2018-89
Manuscript under review for journal Biogeosciences
Discussion started: 20 February 2018

Figure 3

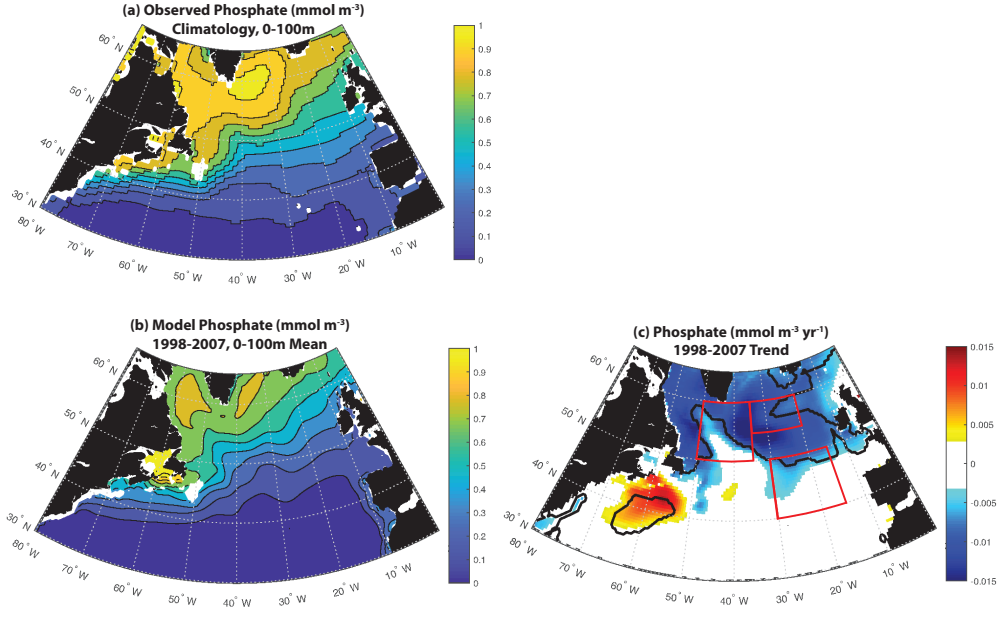

Biogeosciences Discuss., https://doi.org/10.5194/bg-2018-89
Manuscript under review for journal Biogeosciences
Discussion started: 20 February 2018

Figure 4

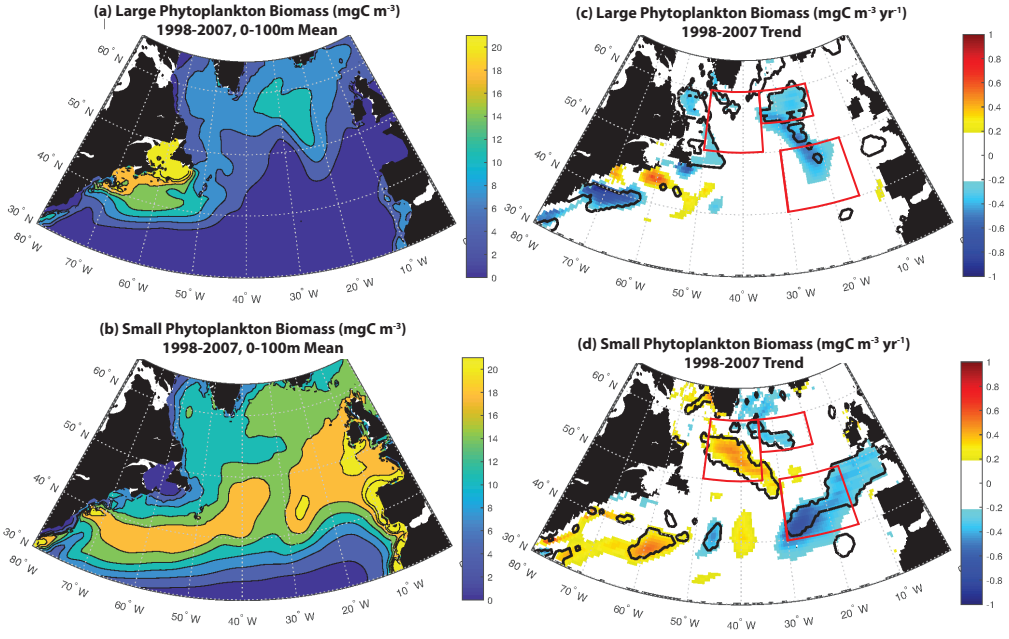

Biogeosciences Discuss., https://doi.org/10.5194/bg-2018-89
Manuscript under review for journal Biogeosciences
Discussion started: 20 February 2018

Figure 5

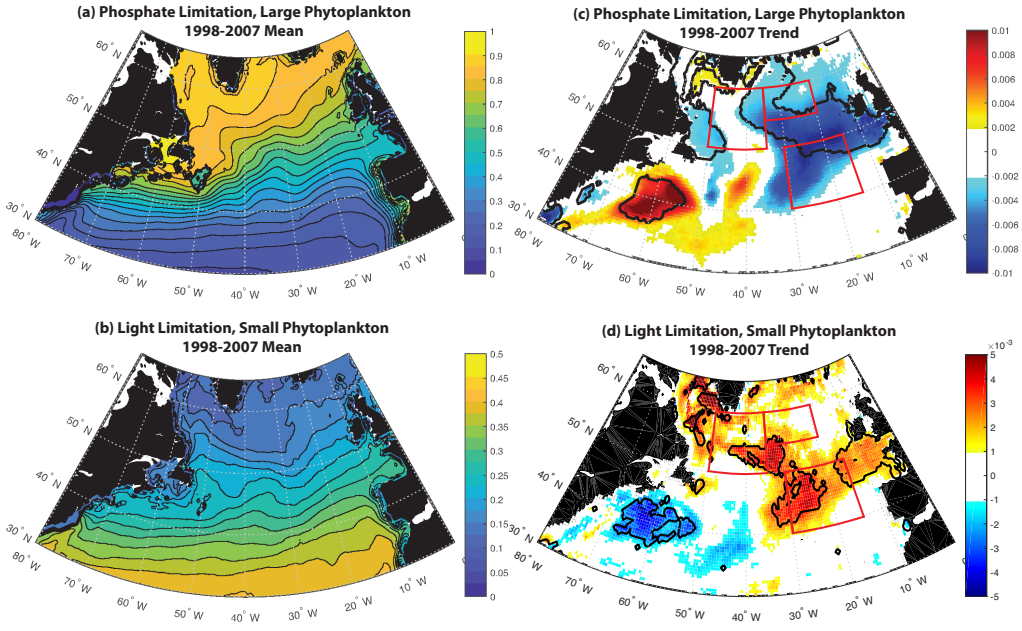

Biogeosciences Discuss., https://doi.org/10.5194/bg-2018-89
Manuscript under review for journal Biogeosciences
Discussion started: 20 February 2018

Figure 6

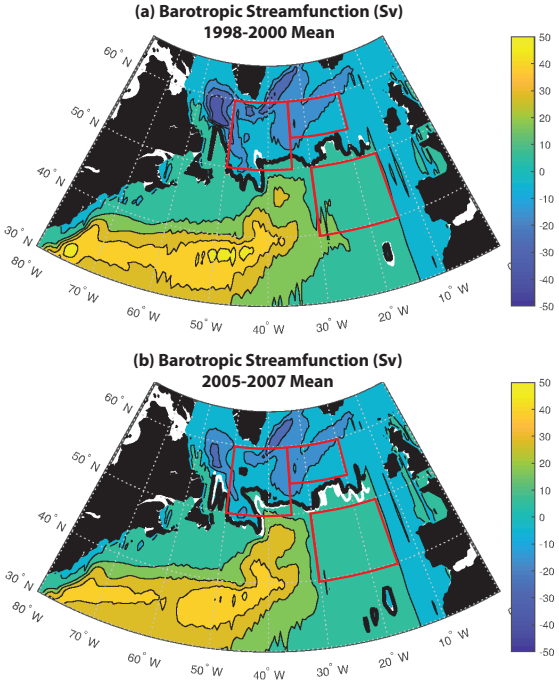

Biogeosciences Discuss., https://doi.org/10.5194/bg-2018-89
Manuscript under review for journal Biogeosciences
Discussion started: 20 February 2018

Figure 7

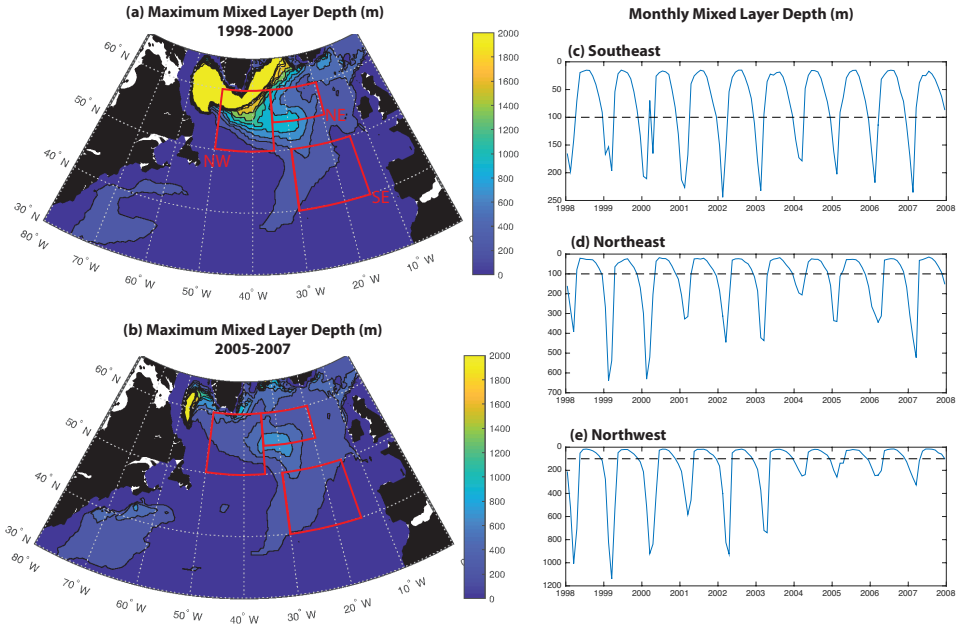

Biogeosciences Discuss., https://doi.org/10.5194/bg-2018-89
Manuscript under review for journal Biogeosciences
Discussion started: 20 February 2018

Figure 8

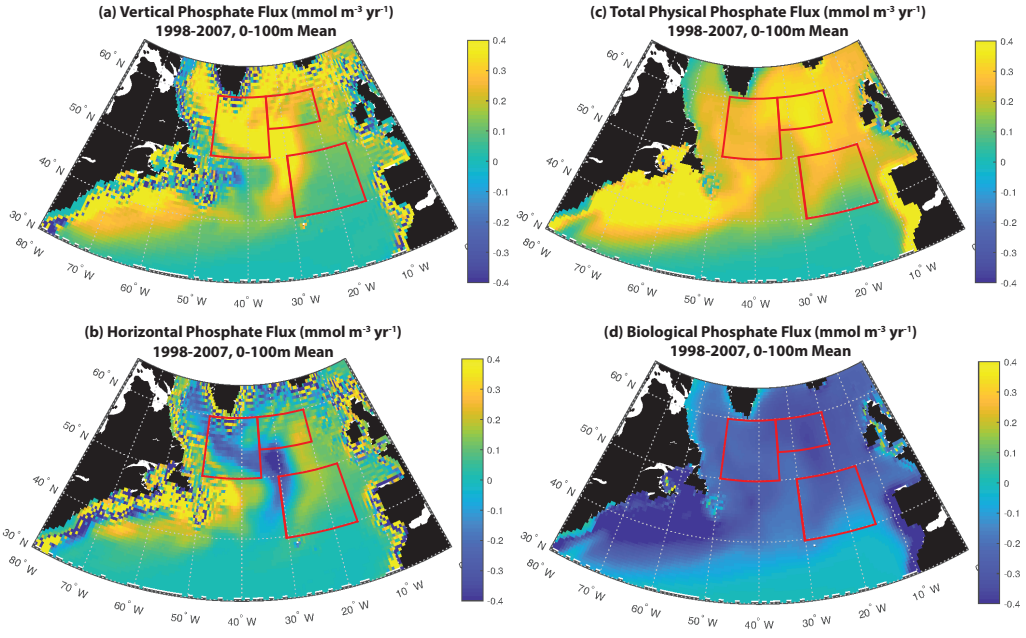

Biogeosciences Discuss., https://doi.org/10.5194/bg-2018-89
Manuscript under review for journal Biogeosciences
Discussion started: 20 February 2018

Figure 9

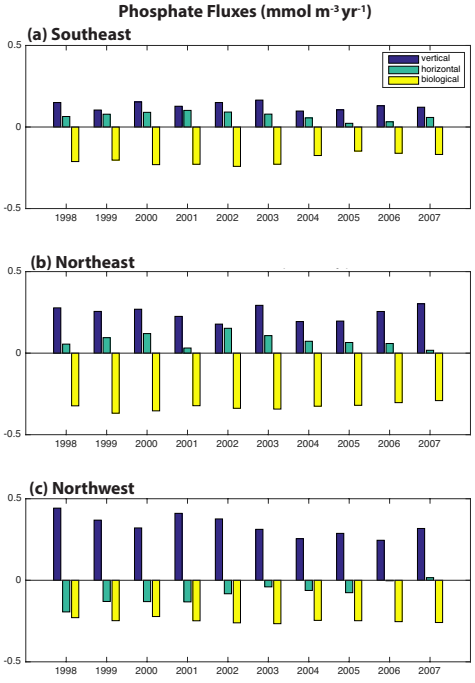

Biogeosciences Discuss., https://doi.org/10.5194/bg-2018-89
Manuscript under review for journal Biogeosciences
Discussion started: 20 February 2018

Figure 10